Journal of Non-Crystalline Solids 357 (2011) 1866–1870

Contents lists available at ScienceDirect

Journal of Non-Crystalline Solids

journal homepage: www.elsevier.com/ locate/ jnoncrysol

Sintering process of amorphous SiO_2 nanoparticles investigated by AFM, IR and Raman techniques

G. Buscarino *, V. Ardizzone, G. Vaccaro, F.M. Gelardi

Department of Physical and Astronomical Sciences, University of Palermo, Via Archirafi 36, I-90123 Palermo, Italy

ARTICLE INFO

Article history:
Received 18 June 2010
Received in revised form 12 November 2010
Accepted 29 November 2010
Available online 1 February 2011

Keywords:
Fumed silica;
Sintering;
Atomic force microscopy;
Raman;
Infrared absorption

ABSTRACT

We report an experimental investigation on the effects of thermal treatments at different temperatures (room–1270 K) and for different duration (0–75 h) on amorphous silica nanoparticles (*fumed silica*) in powder tablet form. Three types of fumed silica are considered, comprising nearly spherical particles of 40 nm, 14 nm and 7 nm mean diameter. The experimental techniques used here are Raman and infrared absorption (IR) spectroscopy together with atomic force microscopy (AFM). Raman and IR spectra indicate that the structure of nanometer silica particles is significantly different with respect to that of a bulk silica glass. In particular, the main differences regard the positions of the IR band peaked at about 2260 cm^{-1}, the Raman R-band peaked at about 440 cm^{-1} and the intensity of the D1 and the D2 Raman lines, related to the populations of 4- and 3-membered rings, respectively. Our data also indicate that, under thermal treatments, the structure of fumed silica samples is significantly changed, gradually relaxing towards that pertaining to ordinary bulk silica. These changes are interpreted here on the basis of the morphological information provided by the AFM measurements and assuming a two-shell structure for the fumed silica primary particles.

1. Introduction

Fumed silica consists in a powder of nonporous amorphous silica nanoparticles produced burning $SiCl_4$ in H_2/O_2 flame [1–5]. The temperatures used in this aerosol process range from 1370 K to 1570 K. The resulting nanoparticles are almost spherical with mean diameters ranging from few nanometers to few tens of nanometers. In the pristine powder the nanoparticles are not rigorously isolated. They can be partially fused in small groups called aggregates. Moreover, isolated particles and/or aggregates usually form weakly bonded bigger groups called agglomerates. Fumed silica materials are widely employed in industrial processes as additives and are present in a lot of commercial products [4,5]. More recently they have attracted an increasing scientific interest, mainly because they manifest many relevant and fascinating properties, which are essentially related to their nanostructured nature. For example, various experimental results have established that fumed silica nanoparticles have a structure significantly different from that of an ordinary bulk silica glass [1–3]. Furthermore, among the peculiar properties of fumed silica, it has been reported that it is particularly reactive to thermal treatment. In fact, upon thermal treatment at temperatures as low as T = 1250 K the system undergoes a relevant solid phase sintering process [6,7]. Due to this process, after prolonged thermal treatment (typically few hundred hours) the material completely loses its nanostructured nature, looking similar to the ordinary silica in many aspects. However, in spite of this similarity, the fully sintered samples have been found to manifest interesting and unexpected features. For example, it has been reported that they exhibit a photoluminescence band in the region from 400 nm to 700 nm under ultraviolet excitation at room temperature. This band represents a new and promising feature which could be used in the future to design more efficient optical and displaying devices [6].

Many general properties of the solid state sintering process discussed above have been recently clarified thanks to our experimental investigation performed by Atomic Force Microscopy (AFM) and Raman techniques [8]. To further investigate this topic, here we report new morphologic (by AFM) and spectroscopic (by Raman and IR) experimental data obtained on a variety of fumed silica materials comprising particles with different sizes which were subjected to thermal treatment at different temperatures. The detailed analysis of the collected spectroscopic data and their comparison with the AFM images give strong evidence of a shell-like structure for the primary nanoparticles and allow a more detailed description at a nanometric level of the sintering process induced by thermal treatment in fumed silica.

2. Experimental details

We considered three different types of fumed silica, whose commercial names are Aerosil® OX 50, Aerosil® 150 and Aerosil® 380. In the sample names reported above numbers indicate the specific surface in m^2/g. These products differ for the distribution of primary nanoparticle diameters, whose mean values are 40 nm, 14 nm and 7 nm, respectively [4]. The as-received powders were compacted using an

* Corresponding author. Tel.: +39 091 6234218; fax: +39 091 6162461.
E-mail address: buscarin@fisica.unipa.it (G. Buscarino).

0022-3093/$ – see front matter © 2011 Elsevier B.V. All rights reserved.
doi:10.1016/j.jnoncrysol.2010.11.114

uniaxial press working at a pressure of 0.3 GPa. It is worth noting that, in accordance with literature data [9,10], this pressure value is unable to induce permanent structural changes in silica nanoparticles. From the self-supporting disks obtained by compacting the pristine powders, the final samples in the form of rectangular tablets with a size of $5\times5\times2$ mm^3 were cut. In particular, a set of 4 samples were produced for each type of fumed silica considered. One of these samples was preserved from any thermal treatment, whereas the remaining three samples were treated at T = 670 K for 2 h, at T = 1270 K for 2 h and finally at T = 1270 K for 75 h.

A bulk a-SiO_2 sample was also considered as a reference to compare the structural properties of fumed silica powders with those of ordinary materials. It consisted in a *Suprasil 1* produced by *Heraeus Quarzglas* with a size of $5\times5\times1$ mm^3.

Tapping mode amplitude modulated AFM [11–15] measurements were acquired with a Multimode V (Veeco Instruments). PointProbe Plus Silicon SPM probes were used, with typical apical diameter of 10 nm. Particular care in assuring the cleanliness of the sample surface is necessary when performing AFM measurements. So we adopted a procedure that consisted in a sequence of three ultrasonic baths in acetone, ethanol and distilled water. Subsequently the samples were positioned in the AFM sample chamber and fluxed with gaseous N_2 for about 10 h. This last step dries the samples, reducing also the thickness of the water film adsorbed on the nanoparticle surfaces.

Raman measurements were acquired at room temperature with a Bruker Ram II FT-Raman spectrometer. The source was a Nd:YAG laser, with a wavelength of 1064 nm and power of 500 mW. The spectral resolution was fixed at 5 cm^{-1}.

IR measurements were acquired at room temperature using a Bruker Vertex 70 Fourier Transform Infrared (FTIR) absorption spectrophotometer, equipped with a MIR light globar source (i.e. a U-shaped silicon carbide piece) and a DLaTGS detector. Spectra were acquired with a spectral resolution of 1 cm^{-1} and were averaged over 200 scans. The absorption spectrum of the empty beam line was subtracted from the spectrum of each sample.

3. Results

In Fig. 1 we report the AFM images acquired on the surface of the fumed silica powder tablets obtained as described in the previous section. They represent a $2\,\mu m\times2\,\mu m$ square portion of the surface, sampled with 512×512 pixels. In these AFM scansions the different particle diameters involved in the three fumed silica types here considered are clearly evident. Furthermore, the images also point out that, even if the powders were pressed to obtain self-supporting samples, large voids still remain among the particles or among their aggregate/agglomerate, conferring to the system a significant degree of porosity.

In order to investigate with higher resolution the morphology of the sample surface, we also obtained images acquired on a length scale of 750 nm × 750 nm sampled with 256×256 pixels, as shown in Fig. 2. The AFM images reported in this figure were acquired on the powder tablets obtained by compacting 7 nm (left column) and 14 nm (right column) nanoparticles. In particular, Fig. 2(a) and (d) refers to untreated samples, Fig. 2(b) and (e) refers to samples thermally treated for 2 h at T = 1270 K, whereas those of Fig. 2(c) and (f) refers to samples thermally treated for 75 h at T = 1270 K. These images indicate that thermal treatments of up to 2 h at T = 1270 K have no evident effect on the morphology of the sample surface, whereas the situation is radically different for the powder tablets treated for 75 h at T = 1270 K. In fact, the images acquired on the surface of these latter samples show that thermal treatment has induced the formation of grains of significantly larger mean size than the diameters of the original primary particles. This experimental evidence proves that a relevant sintering process is actually activated in these samples. At variance, in the samples obtained from 40 nm nanoparticles as a starting material, no morphological alterations

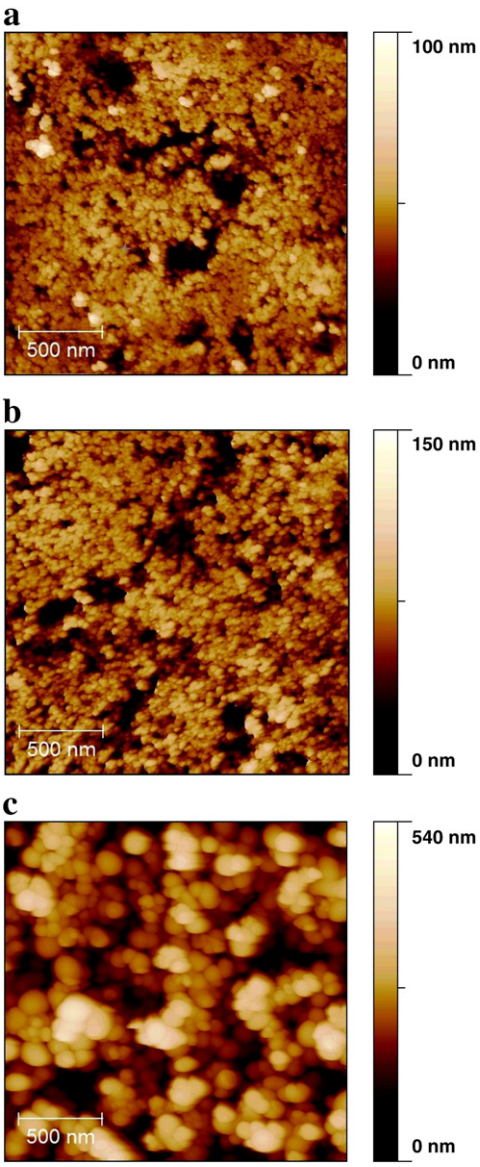

Fig. 1. AFM images acquired on the pristine (untreated) fumed silica powder tablets obtained by compacting nanoparticles with mean diameters (a) 7 nm, (b) 14 nm and (c) 40 nm.

attributable to the sintering process were recognized in any of the considered thermal treatment experiments (data not shown).

As anticipated, to follow the structural changes taking place upon thermal treatment in the three types of fumed silica here considered, Raman measurements were also performed. These data are reported in Fig. 3. In order to make possible a quantitative analysis of the spectra they were normalized to the band at 800 cm^{-1}. This band is assigned to the symmetric stretching of the Si–O–Si groups and it is characterized by the fact that its amplitude and shape hardly change with thermal treatment [16,17]. The data reported in Fig. 3 show that the Raman spectra of the nanostructured samples differ significantly from that of the ordinary bulk silica (also included in the figure, for comparison). Moreover, it is evident that these differences increase on decreasing the mean diameter of the nanoparticles. In particular, two main features are clearly evident. First, the intensities of the D1 (495 cm^{-1}) and D2 (605 cm^{-1}) lines are larger in all the fumed silica samples than in the bulk one, suggesting an enhancement of the number of 4- and 3-membered rings in fumed silica with respect to ordinary materials [3]. Second, the position of the principal band (R-band), assigned to the bending motions of the oxygen atoms in the network, is modified in the

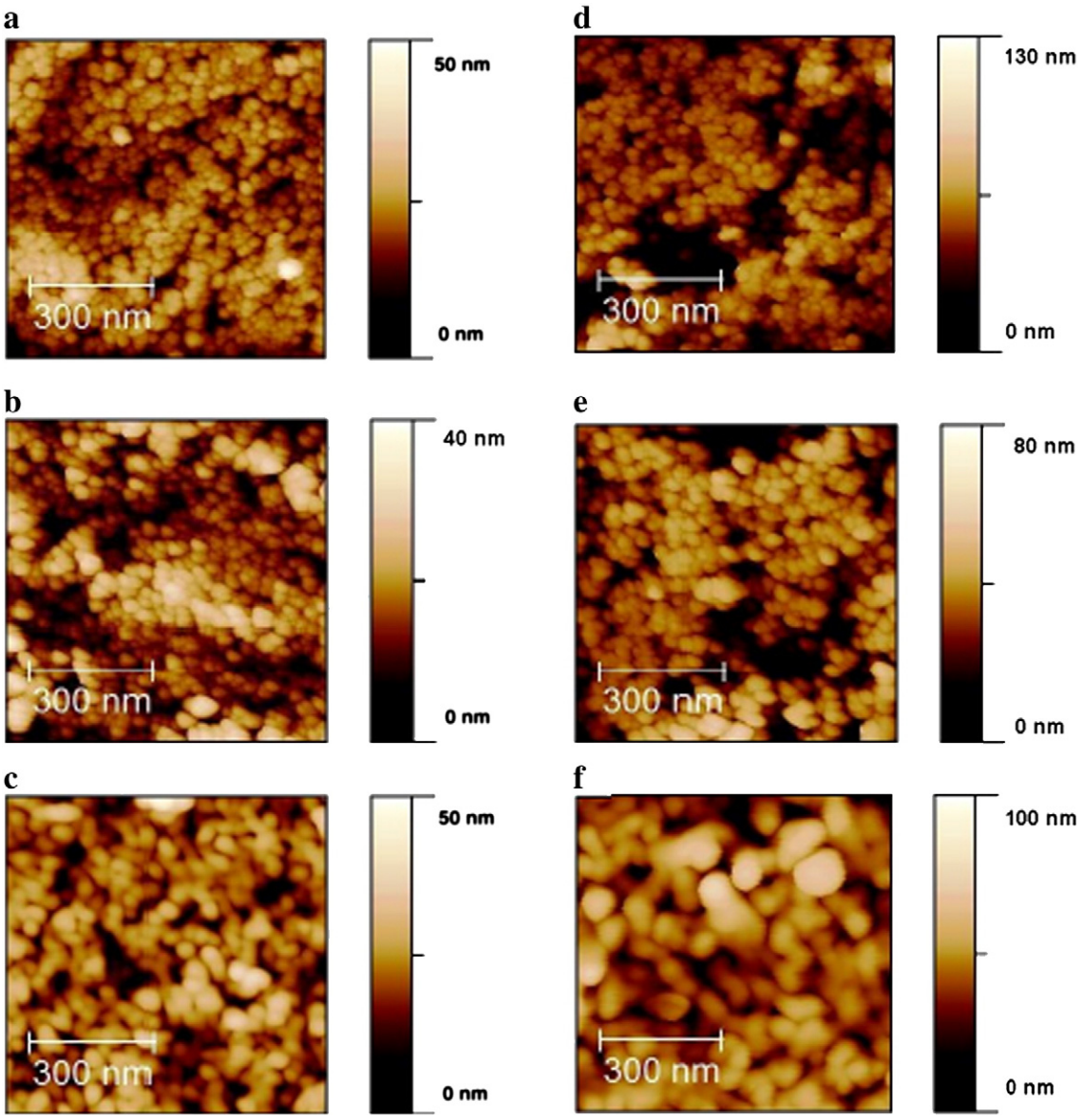

Fig. 2. AFM images acquired on the powder tablets obtained by compacting 7 nm (left column) and 14 nm (right column) nanoparticles. (a) and (d) refer to untreated samples, (b) and (e) refer to samples thermally treated for 2 h at T = 1270 K, whereas (c) and (f) refer to samples thermally treated for 75 h at T = 1270 K.

nanostructured samples with respect to that of the bulk samples, showing a relevant shift towards higher frequencies.

Concerning the effects of thermal treatments our data indicate that they significantly affect the properties of the nanoparticles, allowing a relevant relaxation of the structure. As it can be inferred from Fig. 3 the structural changes become more pronounced on increasing the temperature of the treatment and/or its duration. Two main modifications have been recognized: the shift of the R-band towards lower frequencies and the reduction of the intensity of the D1 and D2 lines. In Fig. 4(a) we report the peak position of the R-band before and after thermal treatments here considered. The last points on the right pertain to the samples treated at T = 1270 K for 75 h. The position of the R-band for the untreated samples shows that the smaller the mean diameter of primary particles, the bigger the observed shift towards high frequencies. Furthermore, it is evident that thermal treatment of up to 2 h at T = 670 K is not able to promote any variation in the peak position, whereas a treatment of the same duration at T = 1270 K significantly changes the R-band, making its spectral position very similar to that characterizing bulk materials. Finally, our data indicate that by further thermally treating the sample at T = 1270 K only minor changes of the peak position are induced with respect to the previous case. Fig. 4(b) shows the intensity of D2 line for the samples before any treatment and after 2 h isochronal treatments at T = 670 K and at T = 1270 K. The last points on the right are the intensities of D2 line for the samples treated for 75 h at T = 1270 K. These data clearly point out that thermal treatments of up to 1270 K for 2 h are not able to induce any detectable effects on the D2 line amplitude. At variance, after 75 h at T = 1270 K the D2 line recovers the spectroscopic features it possesses in bulk materials.

To further characterize the structural changes induced by thermal treatments we have also acquired the IR spectra of the samples under consideration. In particular, these measurements had the main objective to characterize the 2260 cm^{-1} band, which is assigned to an overtone of the strong asymmetric stretching vibration of Si–O–Si bridges. Since this band is correlated with the distribution of the Si–O–Si bond angle [18], its spectroscopic properties give fundamental quantitative information on the structure of the materials and on its evolution upon thermal treatment. The IR spectra we obtained are collected in Fig. 5, except those pertaining to the samples thermally treated for 75 h at T = 1270 K which are omitted for clarity. As it is evident from this figure, the 2260 cm^{-1} band is actually easily recognized in all the spectra. The comparison of the

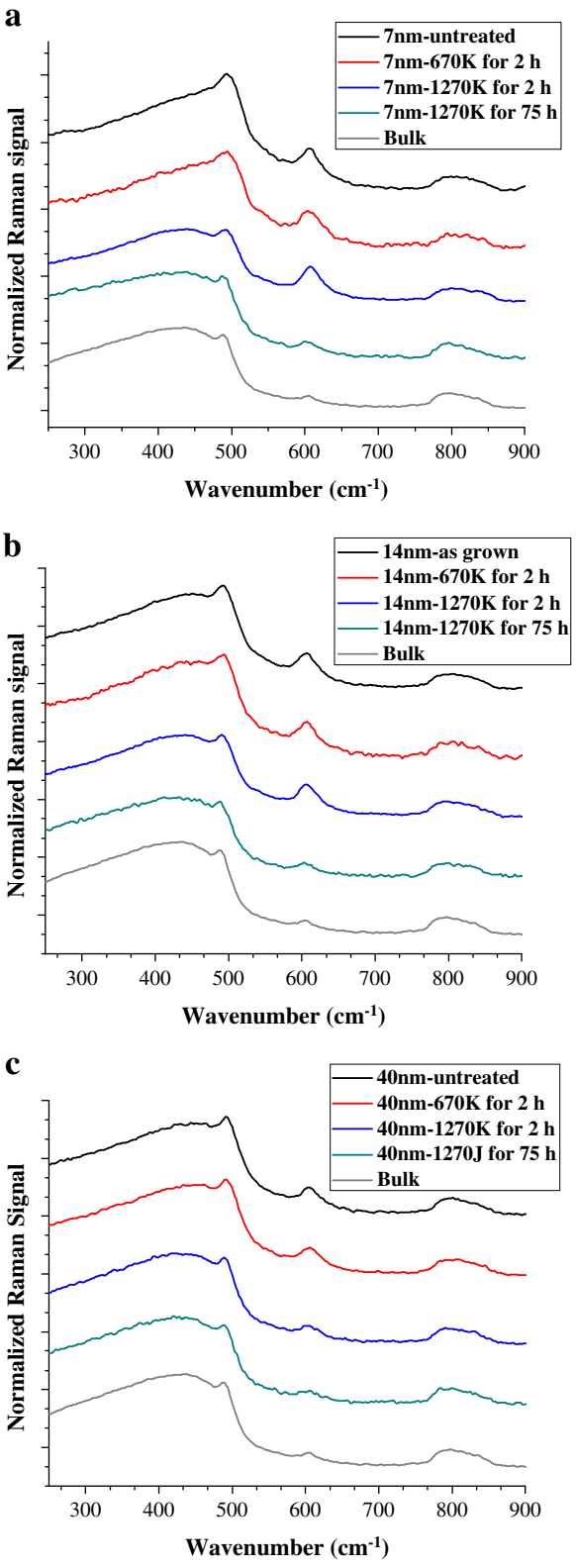

Fig. 3. Raman spectra acquired before and after thermal treatment on the powder tablets obtained by compacting (a) 7 nm, (b) 14 nm and (c) 40 nm nanoparticles. The Raman spectrum of a sample of bulk silica is also included, for reference. The spectra are normalized to the 800 cm^{-1} line and vertically shifted, for clarity.

various spectra points out that the peak position of this band is shifted towards lower wavenumbers in the fumed silica than in ordinary silica. Furthermore, these measurements put forward that the thermal treatments induce a shift towards higher wavenumbers.

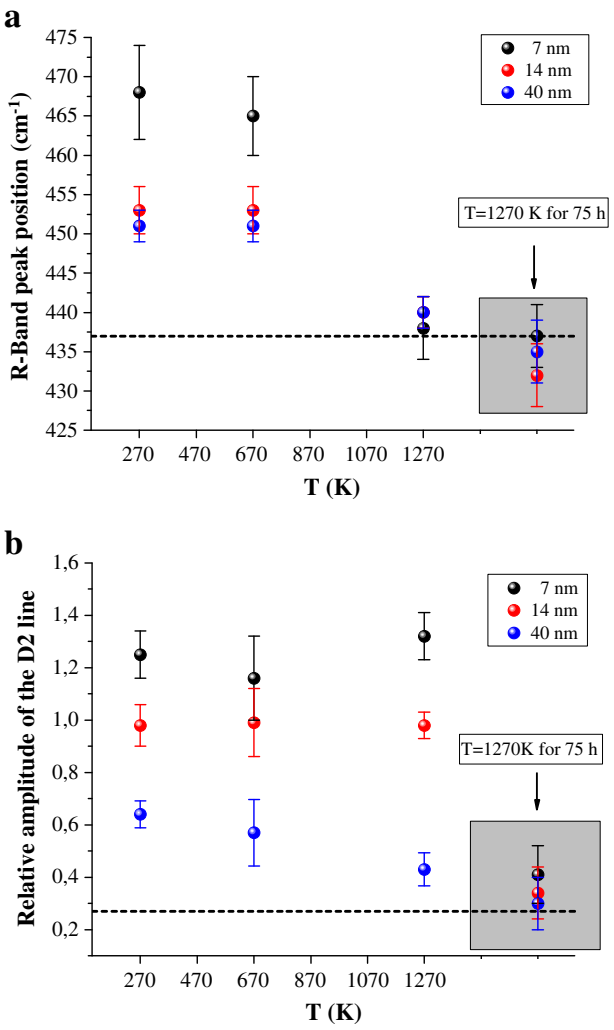

Fig. 4. (a) Peak position of the Raman R-band and (b) the D2 line amplitude estimated in fumed silica powder tablets before and after thermal treatments at T = 670 K and T = 1270 K for 2 h. The points in the grey box show the position of the peak in samples treated for 75 h at T = 1270 K. The dashed lines represent the values obtained in bulk samples.

4. Discussion

The position of the R-band peak is related to the mean Si–O–Si bond angle [19]. As a consequence, its shift towards higher frequencies with respect to the bulk can be interpreted as a smaller mean intertetrahedral bond angle in fumed silica respect to the normal structure of bulk silica. Furthermore, the distribution of the Si–O–Si bond angle and that of the ring sizes are also related to each other. In this respect, generally speaking, our findings could be attributed to a global shift of the ring-size distribution towards smaller rings in nanostructured materials with respect to bulk silica.

Further extending these concepts, one could expect that also the changes occurring in the fumed silica structure upon thermal treatment could be attributed to a global shift of the Si–O–Si bond angle distribution. In these hypotheses one expects that the changes occurring in the R-band position and those pertaining the amplitudes of the D1 and D2 lines should be strictly correlated. In contrast with this expectation the quantitative analysis of the Raman spectra showed in the previous section clearly points out that the modifications of the R-band and that of the D2 lines are uncorrelated. This result shows that the above mentioned hypothesis is incorrect, i.e., the effects of thermal treatment cannot be actually attributed to a global shift of the Si–O–Si bond distribution. As a consequence, a more complex scenario applies and, in

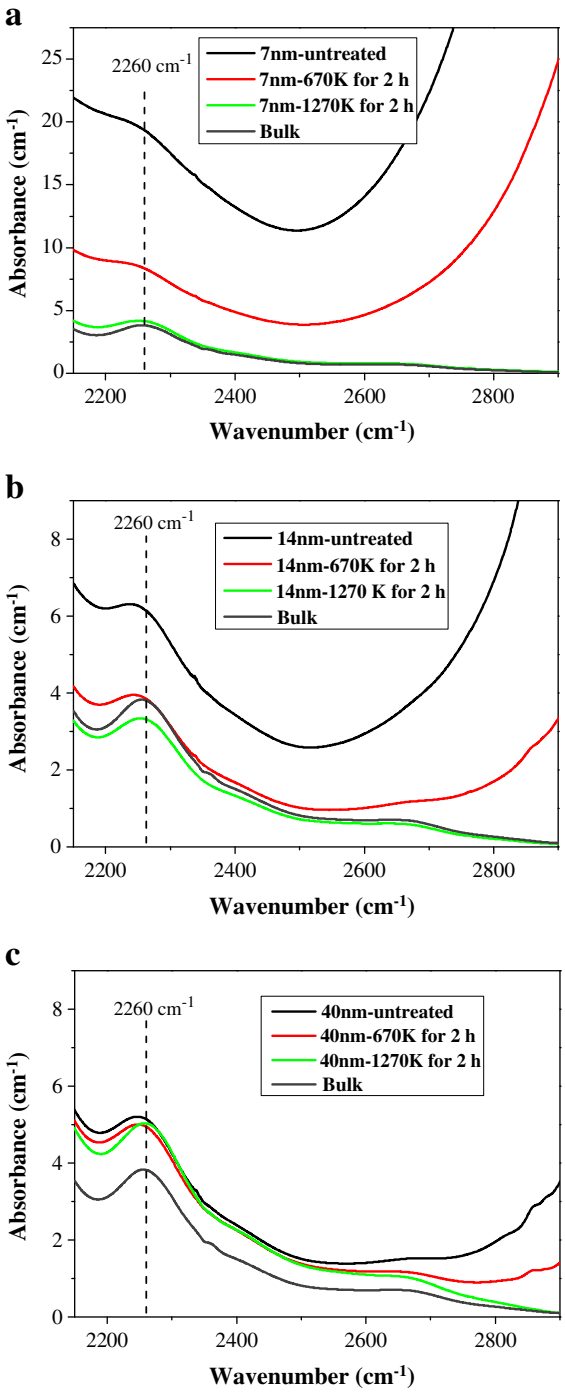

Fig. 5. IR spectra acquired before and after thermal treatment on the powder tablets obtained by compacting (a) 7 nm, (b) 14 nm and (c) 40 nm nanoparticles. The IR spectrum of a sample of bulk silica is also included, for reference.

this respect, the AFM images may help to clarify the mechanisms involved in the modifications of the Raman spectra.

There are many experimental and theoretical evidences [2,20–22] suggesting a shell-like structure for the fumed silica primary particles. In this model each fumed silica nanoparticle is composed by a central region (core) and a surface shell. In both these regions the structure is somewhat different from that of the bulk silica, but to a different extent. In particular, the structure of the external shell is supposed to be strongly strained, and consequently characterized by a dominant concentration of 3- and 4-membered rings, whereas the central region is supposed to be more relaxed. This model may help us to better understand the structural processes taking place in our samples upon thermal treatment. In fact, our data are compatible with the occurrence of two distinct processes affecting different regions of the particle, as explained in the following.

The shift of the R-band peak position induced by the thermal treatment is completed after 2 h at T = 1270 K. However, the AFM images clearly show that after this treatment the morphology of the samples have not changed and there is no evidence of a relevant sintering process. As a consequence, the R-band peak shift upon thermal treatment should be attributed to an ordinary thermal relaxation of the structure of the matrix rather than to the sintering. Furthermore, since the D2 Raman line amplitude is not affected by such a treatment (2 h at T = 1270 K), this relaxation should not involve significantly the surface shell of the particles. In fact, as discussed above, the surface shell is supposed to contain the dominant number of structures responsible for the D1 and D2 lines. Consequently, the structural relaxation responsible for the R-band shift is believed to pertain prevalently to the core of the particles. Similar considerations apply to the observed shift of the 2260 cm^{-1} IR band.

As reported in the previous section, a reduction of the intensity of the D2 line is induced after 75 h of treatment at T = 1270 K. In correspondence of the same treatments the AFM images indicate the occurrence of a relevant sintering process, resulting in a substantial grain growth. Consequently, here we attribute the D2 line amplitude changes observed in our samples to the sintering process which produces a relevant reduction of the specific surface (surface to volume ratio) of the samples and consequently changes sensibly the number of 3- and 4-membered rings of the system.

5. Conclusion

We have found that the Raman spectra of untreated fumed silica samples are very different from that of the bulk silica glass, indicating relevant differences in their microscopic structures. Furthermore, we have found that the thermal treatments of up to 1270 K gradually reduce this differences, making the fumed silica structure more and more similar to that of ordinary bulk materials. In particular we recognized two main modifications: the R-band peak shift towards the lower frequencies and the reduction of intensity of D2 line. Basing on the shell-like model previously proposed for the silica nanoparticles, we attribute the former effect to the thermal relaxation involving mainly the core region of silica nanoparticles, whereas the latter is supposed to arise from the sintering process induced by the thermal treatments in our samples.

References

[1] T. Uchino, et al., Phys. Rev. B 69 (2004) 155409.
[2] A. Stesmans, et al., Phys. Rev. B 77 (2008) 094130.
[3] T. Yamada, et al., J. Phys. Chem. C 111 (2007) 12973.
[4] Basic Characteristics of Aerosil, 4th ed., 2001, Degussa, Frankfurt.
[5] Evonik industries online catalog, http://www.aerosil.com/product/aerosil2010.
[6] T. Uchino, T. Yamada, Appl. Phys. Lett. 85 (2004) 1164.
[7] T. Yamada, T. Uchino, Appl. Phys. Lett. 87 (2005) 081904.
[8] G. Buscarino, V. Ardizzone, G. Vaccaro, S. Agnello, F.M. Gelardi, J. Appl. Phys. 108 (2010) 074314.
[9] T. Uchino, A. Sakoh, J. Phys. Condens. Matter 14 (2002) 11111.
[10] T. Uchino, et al., Phys. Rev. B 67 (2003) 092202.
[11] G. Binning, C.F. Quate, Ch. Gerber, Phys. Rev. Lett. 56 (1986) 930.
[12] R. Garcıa, R. Perez, Surf. Sci. Rep. 47 (2002) 197.
[13] F.J. Giessibl, Rev. Mod. Phys. 75 (2003) 949.
[14] Y. Seo, W. Jhe, Rep. Prog. Phys. 71 (2008) 016101.
[15] A. Yacoot, L. Koenders, J. Phys. D Appl. Phys. 41 (2008) 103001.
[16] F.L. Galeener, Solid State Commun. 44 (1982) 1037.
[17] D.D. Goller, R.T. Phillips, I.G. Sayce, J. Non-Cryst. Solids 355 (2009) 1747.
[18] T. Mohanty, et al., J. Phys. D 36 (2003) 3151.
[19] B. Hehlen, J. Phys. Condens. Matter 22 (2010) 025401.
[20] A. Stesmans, K. Clémer, V.V. Afanas'ev, Phys. Rev. B 72 (2005) 155335.
[21] T. Uchino, Phys. Rev. B 69 (2004) 155409.
[22] A. Roder, et al., J. Chem. Phys. 114 (2001) 7602.